Optics Letters

Flexible GaN-based ultraviolet microdisk lasers on PET substrate

Peng Gu, Shuai Yang, Lilong Ma, Tao Yang, Xin Hou, Yang Mei,* Leiying Ying, Hao Long, and Baoping Zhang

Laboratory of Micro/Nano-Optoelectronics, Department of Micro Electronic and Integrated Circuits, Xiamen University, Xiamen 361005, China
**meiyang@xmu.edu.cn*

Received 1 June 2023; revised 9 July 2023; accepted 9 July 2023; posted 12 July 2023; published 27 July 2023

Flexible optoelectronics is a technique for fabricating optoelectronic devices on a flexible substrate. Compared with conventional devices, flexible optoelectronic devices can be used in more complex working environments benefiting from the mechanical flexibility. Herein, for the first time to the best of our knowledge, a flexible GaN-based microdisk laser on a polyethylene terephthalate (PET) substrate in the ultraviolet A (UVA) range was demonstrated by using thin film transfer process based on laser lift-off (LLO). The lasing wavelength is 370.5 nm with a linewidth of 0.15 nm and a threshold power density of 200 kW/cm^2. Additionally, a distributed Bragg reflector (DBR) was deposited on the backside of the microdisk as the bottom mirror between GaN microdisk and PET substrate, which can provide better mode confinement inside the microdisk and increases the oscillation intensity. The lasing wavelength of the flexible laser shows a 2-nm redshift under different bending curvature of the substrate, which is promising for applications such as mechanical sensing. © 2023 Optica Publishing Group

https://doi.org/10.1364/OL.496680

Flexible optoelectronic devices have recently attracted substantial attention due to their deformable characteristics. Compared with conventional optoelectronic devices, they can be applied in more extensive fields such as artificial photonic skin, diagnosis of diseases, deformable displays, and mechanical sensing [1,2]. GaN-based semiconductor materials are suitable for fabricating optoelectronic devices which benefit from their continuous adjustable emission wavelength from 200 nm to 1.7 µm [3]. However, due to the limitation caused by the lattice mismatch and high growth temperature (>1000°C) [4], the epitaxial layers of GaN-based materials usually need to be grown on a highly stable rigid substrate such as Si, sapphire, SiC, GaN, etc. This poses a challenge for the fabrication of GaN-based flexible optoelectronic devices. To overcome the difficulties, many research groups have proposed different solutions which can be summarized into two conceptually different ways. The first approach is to form the nanostructures such as nano/microwire or nanopillar on a flexible substrate by low-temperature molecular beam epitaxy (MBE) [5,6]. Another proven method is transferring the GaN-based membrane onto a flexible substrate, which can be realized by wafer bonding and peeling of the original substrate through laser lift-off (LLO) or the wet etching method [7,8]. More recently, Fang Ren *et al*. also reported the growth of high-quality GaN films on graphene (Gr)/glass through van der Waals epitaxy, enabling the much easier transfer of a GaN-based membrane to a flexible substrate [9]. After transferring the film from the rigid substrate onto a flexible conducting polymer substrate, flexible LEDs were successfully fabricated.

The substrate transferring technology can also be applied to fabricate GaN-based flexible lasers, although there are only a few successful reports. In 2019, Kwai Hei Li *et al*. fabricated flexible GaN-based microdisk lasers on polydimethylsiloxane (PDMS) substrate by using the LLO process and the lasing wavelength is 440.6 nm [10]. In 2021, Peng Hu *et al*. fabricated a microtubular cavity by electrochemical etching and then encapsulated the microtubule with a flexible PDMS substrate, and lasing at ∼419.03 nm with linewidth of 0.07 nm was realized [11]. Among the lasers with different wavelengths, lasers in the ultraviolet (UV) band are attracting great attention at the present because of their promising application potential in the field of laser radar, photoresist curing, bioagent detection, sterilization and disinfection, optical communication, and sensors. Currently, these applications, especially the UV sensors, are required to operate under complex working conditions [12]. If we can combine the UV micro laser with a flexible substrate, the high flexibility will allow devices to be promising for a much wider range of applications. However, research on GaN-based flexible lasers in the UV band is still unreported.

In this study, for the first time to the best of our knowledge, flexible GaN based microdisk lasers in the ultraviolet A (UVA) range were successfully fabricated. By using the LLO process, the GaN-based membranes containing InGaN/GaN QWs were transferred onto the transparent and flexible polyethylene terephthalate (PET) substrate. A dielectric distributed Bragg reflector (DBR) was deposited on the backside of the microdisk as the bottom mirror between the GaN microdisk and PET substrate, which can provide better mode confinement and increase the oscillation intensity. Lasing in the UVA band was realized under the optically pumping condition. The lasing wavelength was 370.5 nm with a linewidth of 0.15 nm, and the threshold power density was 200 kW/cm^2. Moreover, the lasing characteristics were studied under various bending radius and a peak energy shift was regularly accomplished by a change of the bending

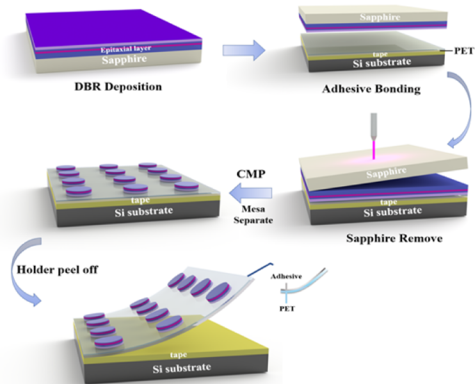

Fig. 1. Fabrication process of the flexible microdisk lasers on PET.

curvature. Such a tunable property of the wavelength under different bending curvatures enables the flexible lasers to play a more important role in the fields of skin sensors and wearable devices.

The epitaxial wafer used in this work was grown on (0001)-oriented sapphire substrate by metal–organic chemical vapor deposition (MOCVD). First, a 2-μm unintentionally doped GaN layer was grown on sapphire substrate followed by a 2-μm-thick n-GaN layer. Then the active region containing five pairs of $In_{0.1}Ga_{0.9}N/GaN$ (2/6 nm) multi-quantum wells and a 20 nm-thick p-AlGaN electron blocking layer as well as a 93-nm thick p-GaN layer were sequentially grown. The epi-structure here with Si and Mg doping can also allow us to fabricate electrically injected flexible microdisk lasers in the future [13]. The fabrication process of the flexible GaN based microdisk lasers is illustrated in Fig. 1. A dielectric DBR containing 12.5 pairs of TiO_2/SiO_2 was first deposited on the epitaxial wafer. Then the sample was flip chip bonded on a transparent PET substrate through adhesive bonding. The PET substrate here was adhered to a temporary Si substrate in advance to support the GaN membrane during the following LLO process. The sapphire substrate was subsequently removed by LLO, and the epitaxial film was thinned down to a thickness of ~800 nm by chemical mechanical polishing (CMP). The mesa of the microdisks was formed by inductively coupled plasma (ICP) etching, and the diameter of the microdisks was 25 μm. At last, the temporary Si holder was removed.

Figures 2(a) and 2(b) show the photograph and scanning electron microscopy (SEM) image of the flexible microdisk lasers under bending condition. The film shows good recoverability after being bent under large curvature for more than 200 times. The single device as well as the microdisk array can maintain their integrity, which proves the high stability of the flexible microdisk lasers. Figure 2(c) shows the atomic force microscopy

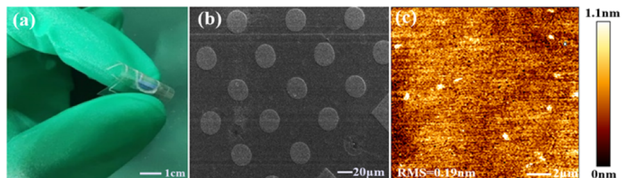

Fig. 2. (a) Photo of the flexible microdisk lasers under bending. (b) SEM image of microdisks after bending. (c) AFM image of the sample after CMP.

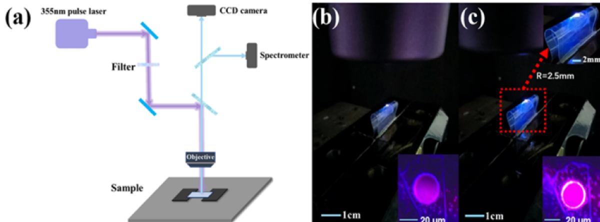

Fig. 3. (a) Schematic diagram of micro-PL measurement system. Nearfield images of a microdisk (b) below and (c) beyond threshold.

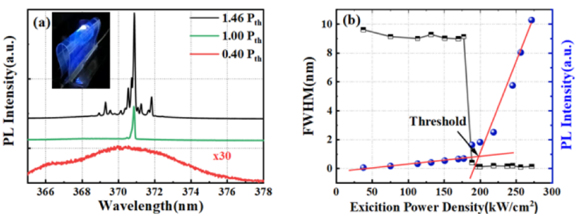

Fig. 4. (a) Emission spectra of a microdisk below and beyond threshold and (b) emission intensity and linewidth of the microdisk laser as a function of excitation power density.

(AFM) image of the top surface of the microdisk after CMP. The root mean square (rms) is only 0.19 nm on a 10×10-μm^2 area, which means that the microdisk is featured with an atomic-level smooth surface. This is important to reduce the scattering loss of the microcavity and reduce the lasing threshold [14].

As shown in Fig. 3(a), the optical properties of the flexible microdisk lasers were evaluated by a micro-photoluminescence (PL) measurement system at room temperature. The devices were excited by a 355-nm pulsed laser through the objective lens with a repetition rate of 15 kHz and pulse duration width of 1 ns. The light emitted by the device was then collected by the same objective lens and guided to the spectrometer for measurement.

The circular excitation laser spot was focused on the sample surface with a diameter of 27 μm. The primary modes in a microdisk cavity originate from whispering gallery modes (WGMs) which are produced by the total internal reflection of the light traveling around the circumference of the disk [15]. Figures 3(b) and 3(c) show the photographs of the microdisk under excitation powers of $0.4P_{th}$ and $1.46P_{th}$, respectively, and the bending radius (R) is 2.5 mm. The inset shows the corresponding near field image. The brightness of the microdisk is much stronger under $1.46P_{th}$, and the optical field is mainly distributed near the edge of the microdisk, which is a signature of the oscillation of the WGMs. The PL spectra of the microdisk laser is shown in Fig. 4(a). Under the excitation energy below the lasing threshold ($0.4P_{th}$), the PL spectrum shows a broad emission peak due to spontaneous emission. As the excitation energy is increased beyond the lasing threshold ($1.46P_{th}$), the spectrum mainly shows narrow peaks which is dominated by the WGMs at ~370.5 nm. The lasing wavelength is 370.5 nm in the UVA band, which is the shortest wavelength for flexible GaN-based lasers compared with other studies. Figure 4(b) shows the emission intensity and linewidth of the microdisk laser as a function of excitation power density. As the excitation power density increases beyond the lasing thresholds, the emission intensity increases sharply together with an abrupt narrowing of the linewidth, further proving the lasing action. The threshold was estimated to be ~200 kW/cm^2.

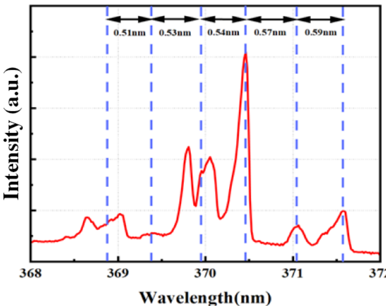

Fig. 5. Lasing spectrum of the microdisk at an excitation power density of 260 kW/cm^2.

To estimate the free spectral range (FSR) of the first radial order WGMs, the following equation can be used [16]:

$$\Delta\lambda = \frac{\lambda^2}{\pi D \cdot ngroup}, \quad (1)$$

where D is the diameter of the microdisk; λ is the mode wavelength; and $ngroup$ is the group effective index of refraction, which can be calculated using the following equation:

$$n_{group} = n_{eff} - \left(\frac{dn_{eff}}{d\lambda}\right) \cdot \lambda, \quad (2)$$

where n_{eff} is the effective refractive index and $dn_{eff}/d\lambda$ is the dispersion. Generally, the group is 20–30% higher than the effective index [17], so we estimated the value of $ngroup$ to be ~3.3 at 370.5 nm (n_{eff}~ 2.6) [18]. Using $D = 25.0$ µm, the predicted FSR is ~0.53 nm at 370.5 nm, which is consistent with the experimental values, as shown in Fig. 5. Peaks which do not match the first radial order mode come from higher-order modes. As the pumping energy is increased, higher-order WGMs can be supported simultaneously for lasing, which can also contribute to the luminous power of the laser.

The dielectric DBR between the microdisk and the PET substrate is expected to be helpful for the mode confinement and suppression of mode leakage to the PET substrate. The mode field distribution of the microdisk along the vertical direction is calculated by using the finite element method (FEM) to investigate the effect of the bottom DBR on luminous properties, and the results are shown in Fig. 6. It can be clearly observed that the optical field intensity of the sample with the bottom DBR mirror is improved compared with that of the sample with no mirror. The high reflectivity of DBR allows the optical field to be better confined within the microdisk.

To study the performance of the flexible microdisk lasers under different bending conditions, the lasing wavelength of the microdisk was measured by adjusting the bending curvature of the PET substrate. The devices were folded upward through different radius of curvature (R) of 6.5 mm, 4 mm, and even 2.5 mm. The lasing peak of the microdisk laser shifted from 369.6 nm to 371.6 nm when the curvature of the film was increased from 0 to 0.4 mm^{-1}, as shown in Fig. 7(a). For Ga-polar InGaN/GaN QWs grown along the c axis, the spontaneous polarization (P^{sp}), piezoelectric polarization (P^{pz}), and polarization induced electrical field in the QW can be determined as follows [19]:

$$P^{sp}_{In_xGa_{1-x}N} = -0.042x - 0.034(1-x) + 0.038x(1-x), \quad (3)$$

$$P^{pz}_{In_xGa_{1-x}N/GaN} = 0.148x - 0.0424x(1-x) \quad (4)$$

$$E_w = -\frac{l(P^{sp}_{In_xGa_{1-x}N} + P^{pz}_{In_xGa_{1-x}N/GaN} - P^{sp}_{GaN})}{\varepsilon_0(\varepsilon_{GaN} d + \varepsilon_{InGaN} l)}, \quad (5)$$

where l and d are the thickness of the GaN barrier layer and the InGaN well layer, respectively; ε_0 and ε_{GaN} are vacuum dielectric constant and relative dielectric constant of GaN; ε_{InGaN} is the dielectric constant of $In_xGa_{1-x}N$ which is calculated by linear interpolation of the value of the relative dielectric constant of InN and GaN. The value of the dielectric constant and the P^{sp}_{GaN} are presented in Table 1 [15].

In this study, the indium content is 0.1, and the polarization induced electric field is calculated to be 0.61 MV/cm, which is similar to the result calculated in other literature (0.57 MV/cm) [20]. The small built-in electric field means that the incline of the energy band of the InGaN QW is negligible [21], as shown in the schematic diagram in Fig. 7(b). After the sample is bent upward, the devices are subjected to additional tensile stress. The compressive stress in the QW layers caused by the lattice mismatch between InGaN and GaN can be compensated [22]. When an external tensile stress was applied, the additional piezo-electric field caused by external tensile stress is in the same direction as the spontaneous polarization electric field [23]. This will induce the increment of the energy band of the QWs, as schematically shown in Fig. 7(c). With the increase of the bending curvature, the inclination of the energy band will be more remarkable. This causes a decreased effective bandgap of the QWs and then the gain spectral redshift of the microdisk lasers. The values of the stresses transmitted to the active region

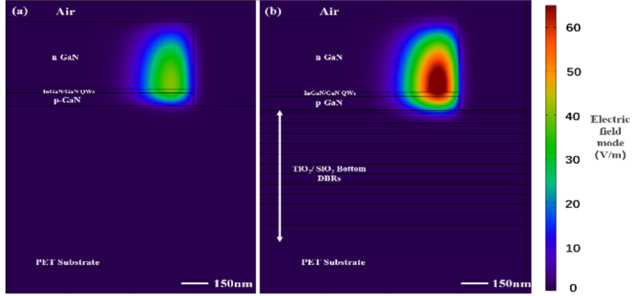

Fig. 6. Mode field distribution of the vertically confined WGMs calculated by FEM.

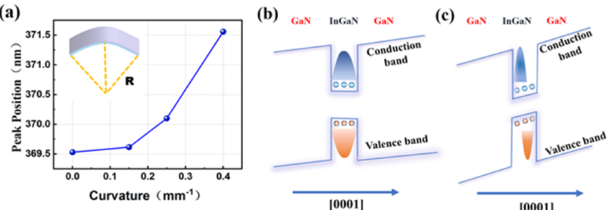

Fig. 7. (a) Peak position of the microdisk laser as a function of curvature. (b) Schematic diagram of the quantum well energy band without bending and (c) under upward bending conditions.

Table 1. Value of the Dielectric Constant

ε_0 (F/m)	$8.854187817 \times 10^{-12}$
ε_{GaN}	8.9
ε_{InN}	15.28
ε_{InGaN}	$15.28x + 8.9(1-x)$
P^{sp}_{GaN} (C/m^2)	0.034
ε_0 (F/m)	$8.854187817 \times 10^{-12}$

are complex to calculate. Thus, here is only a qualitative description of the redshift of the energy band caused by stress. Note that Li *et al.* reported the blueshift of the lasing wavelength of a GaN based microdisk laser (diameter ∼1 µm) under bending condition, which is caused by the decreased effective radius and optical path length for one round trip in a bended disk-shape cavity [10]. However, this is not the case in this study because the diameter of the microdisk is much larger, that is, 25 µm, and the mode wavelength is less sensitive to the deformation of the cavity shape. The redshift of the lasing wavelength of the device can be explained by the redshift of the peak-gain, and then the mode hopping of the WGMs with longer wavelength. Combined with the small mode spacing due to the large size of the device, the cavity modes with longer wavelength starts to lase under bending condition (gain is redshifted and the mode-hopping is raised). For these reasons, we can observe the redshift from the lasing spectrum under different curvatures.

In summary, optically pumped flexible GaN-based UVA microdisk lasers were fabricated for the first time. The microdisks were transferred onto a flexible and transparent PET substrate by LLO. The lasing wavelength of the device is 370.5 nm with a threshold power density of 200 kW/cm^2 at room temperature. The lasing action of the flexible microdisks can be well maintained after bending the substrate to a curvature radius as small as 2.5 mm. The redshift of peak position accompanied with the increasing curvature demonstrates wavelength-tunable characteristics of the flexible lasers. This work can be promising for applications of GaN-based lasers and flexible optoelectronic devices in the field of mechanical sensors.

Funding. National Key Research and Development Program of China (No. 2017YFE0131500); National Natural Science Foundation of China (No. 62104204, U21A20493 62234011, 62174140); President's Foundation of Xiamen University (No. ZK1044).

Acknowledgments. The authors also thank Huan Xu, Yachao Wang, and Yanhui Chen for providing theoretical support.

Disclosures. The authors declare no conflicts of interest.

Data availability. Data underlying the results presented in this paper are not publicly available at this time but may be obtained from the authors upon reasonable request.

REFERENCES

1. S. Y. Lee, K.-I. Park, C. Huh, M. Koo, H. G. Yoo, S. Kim, C. S. Ah, G. Y. Sung, and K. J. Lee, Nano Energy **1**, 145 (2012).
2. W.-S. Choi, H. Cui, S.-H. Park, S. O. Cho, J. K. Lee, T. S. Kim, J. H. Song, and T. Jeong, Mater. Lett. **165**, 252 (2016).
3. W. Sha, Q. Hua, J. Wang, Z. Cong, X. Cui, K. Ji, X. Dai, B. Wang, W. Guo, and W. Hu, ACS Appl. Mater. Interfaces **14**, 3000 (2022).
4. X. Chen, J. Dong, C. He, L. He, Z. Chen, S. Li, K. Zhang, X. Wang, and Z. L. Wang, Nano-Micro Lett. **13**, 67 (2021).
5. H. Sun and X. Li, Phys. Status Solidi A **216**, 1800420 (2018).
6. C. Zhao, T. K. Ng, R. T. ElAfandy, A. Prabaswara, G. B. Consiglio, I. A. Ajia, I. S. Roqan, B. Janjua, C. Shen, J. Eid, A. Y. Alyamani, M. M. El-Desouki, and B. S. Ooi, Nano Lett. **16**, 4616 (2016).
7. M. Asad, Q. Li, M. Sachdev, and W. S. Wong, Nano Energy **73**, 104724 (2020).
8. J. Zhu, X. Zhou, L. Jing, Q. Hua, W. Hu, and Z. L. Wang, ACS Nano **13**, 13161 (2019).
9. F. Ren, B. Y. Liu, and Z. L. Chen, *et al.*, Sci. Adv. **7**, eabf5011 (2021).
10. K. H. Li, Y. F. Cheung, and H. W. Chi, ACS Appl. Electron. Mater. **1**, 1112 (2019).
11. P. Hu, Y. Li, S. Zhang, Y. Zhang, Z. Tian, and F. Yun, Crystals **11**, 1251 (2021).
12. G. Dubourg and M. Radovic, ACS Appl. Mater. Interfaces **11**, 6257 (2019).
13. Y. Mei, M. Xie, T. Yang, X. Hou, W. Ou, H. Long, L. Ying, Y. Liu, G. Weng, S. Chen, and B. Zhang, ACS Photonics **9**, 3967 (2022).
14. Y. Mei, M. Xie, H. Long, L. Ying, and B. Zhang, J. Lightwave Technol. **40**, 2952 (2022).
15. C. E. Dreyer, A. Janotti, C. G. Van de Walle, and D. Vanderbilt, Phys. Rev. X **6**, 021038 (2016).
16. G. Zhu, J. Li, J. Li, J. Guo, J. Dai, C. Xu, and Y. Wang, Opt. Lett. **43**, 647 (2018).
17. A. C. Tamboli, E. D. Haberer, R. Sharma, K. H. Lee, S. Nakamura, and E. L. Hu, Nat. Photonics **1**, 61 (2007).
18. E. Ejder, Phys. Status Solidi A **6**, 445 (1971).
19. V. Fiorentini, F. Bernardini, and O. Ambacher, Appl. Phys. Lett. **80**, 1204 (2002).
20. L. Dong, J. V. Mantese, V. Avrutin, Ü Özgür, H. Morkoç, and S. P. Alpay, J. Appl. Phys. **114**, 043715 (2013).
21. M. Feneberg and K. Thonke, J. Phys.: Condens. Matter **19**, 403201 (2007).
22. Y. Mei, Y. H. Chen, L. Y. Ying, A. Q. Tian, G. E. Weng, L. Hao, J. P. Liu, and B. P. Zhang, Opt. Express **30**, 27472 (2022).
23. J. Mo, Q. Hua, W. Sha, M. Yao, J. Wang, L. Wan, J. Zhai, T. Lin, and W. Hu, Superlattices Microstruct. **155**, 106926 (2021).